

# Charge Transfer Complexes of Discotic Liquid Crystals: A Flexible Route to a Wide Variety of Mesophases

Paul H. J. Kouwer,<sup>†</sup> Wolter F. Jager, Wim J. Mijs, and Stephen J. Picken\*

Delft University of Technology, Polymer Materials and Engineering, Julianalaan 136, 2628 BL Delft, The Netherlands

Received October 25, 2001; Revised Manuscript Received March 6, 2002

**ABSTRACT:** We have prepared a new discotic nematogen, bearing one functional tail and five methoxy substituents. The corresponding side chain polymers, prepared via a polymer analogous esterification reaction, exhibited  $N_D$  phases from 50 °C until degradation above 200 °C. Addition of equimolar amounts of various trinitrofluorenone-based acceptors to the mesogen resulted in the formation of charge transfer complexes with a variety in liquid crystalline properties. Depending on the acceptor, different columnar and nematic phases are induced, including the recently discovered nematic lateral phase. The liquid crystalline properties were investigated with differential scanning calorimetry, optical polarizing microscopy, and extensive X-ray diffraction (XRD).

## Introduction

Since their discovery in the late 1970s,<sup>1</sup> discotic liquid crystals (DLCs) have received growing attention.<sup>2</sup> Interest has increased due to various possible applications, e.g., as compensation layers in LCD technology<sup>3a,b</sup> and for one-dimensional conduction.<sup>3c</sup> However, before DLCs may be applied, knowledge of and control over the mesomorphic properties, i.e., the phase behavior and transition temperatures of the materials, is crucial. Therefore, a wide range of flat and rigid molecules, usually substituted by multiple flexible tails, have been synthesized and investigated for their liquid crystalline properties.<sup>2a</sup> It has been shown that the phase behavior can be controlled by chemical modification of the size and nature of the core, by the type and length of flexible tails, or by an asymmetric substitution of the core.<sup>2a</sup>

Liquid crystalline organization of disk-shaped mesogens results in the formation of various nematic and columnar phases. Several nematic phases have been reported (see Figure 1). Two of the nematic phases are well established. In the nematic discotic ( $N_D$ ) phase,<sup>4</sup> which was found just after the discovery of discotic liquid crystals, the molecules only possess orientational order. The nematic columnar ( $N_{Col}$ ) phase, found 10 years later,<sup>5,6</sup> is characterized by a local columnar stacking of the molecules and a nematic arrangement of the columns. Recently, we have discovered a third nematic phase where the disk-shaped molecules aggregate into large disk-shaped superstructures, and these aggregates show a nematic arrangement. This phase is referred to as the nematic lateral ( $N_L$ ) phase due to the strong lateral interactions between the mesogens.<sup>7</sup> Note that for the superstructures of the  $N_L$  and the  $N_{Col}$  phase the local organization can be very high, but the long-range positional order is absent, i.e., a nematic phase.

For disk-shaped molecules, the nematic phase is rather uncommon. Much more frequently observed are

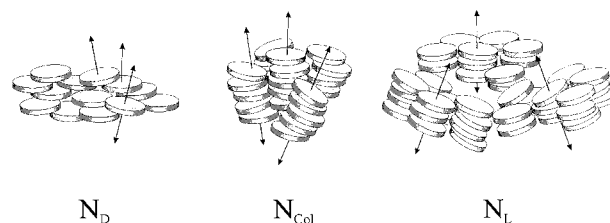


**Figure 1.** Nematic mesophases:  $N_D$  = nematic discotic;  $N_{Col}$  = nematic columnar;  $N_L$  = nematic lateral.

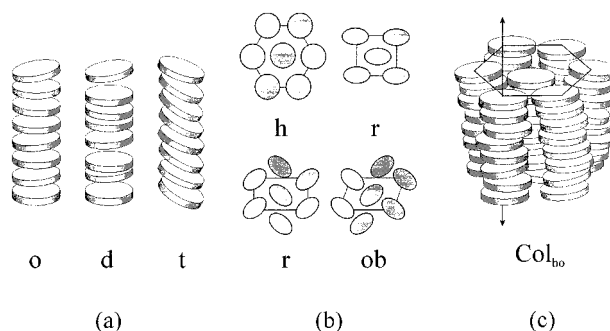


**Figure 2.** Columnar mesophases: (a) side view of the columns: ordered (o), disordered (d), or tilted (t); (b) top view (ellipsoids are tilted disks): hexagonal (h), rectangular (r), or oblique (ob); (c) example: columnar hexagonal ordered ( $Col_{ho}$ ).

the columnar ( $Col_X$ ) phases. Here, the molecules are stacked into columns, and the columns possess a long-range two-dimensional organization. The organization within the columns and between the columns is indicated by suffixes (see Figure 2).

Apart from changing the chemical composition of DLCs, other ways to manipulate their phase behavior have been explored. Recently, we reported an increased liquid crystalline diversity that was obtained by attaching the mesogens to a polymer backbone.<sup>7a,8</sup> Such polymers showed mesophases that were not observed in the corresponding low molar mass mesogens. An additional advantage of polymers is that, in general, crystallization is suppressed, and hence, a broad temperature window for mesophases is obtained. Moreover, a desired liquid crystalline texture can be frozen in

<sup>†</sup> Present address: Department of Chemistry, University of Hull, Cottingham Road, Hull, HU9 1HD, United Kingdom. E-mail: P.H.J.Kouwer@hull.ac.uk.

\* Corresponding author. E-mail: S.J.Picken@tnw.tudelft.nl.

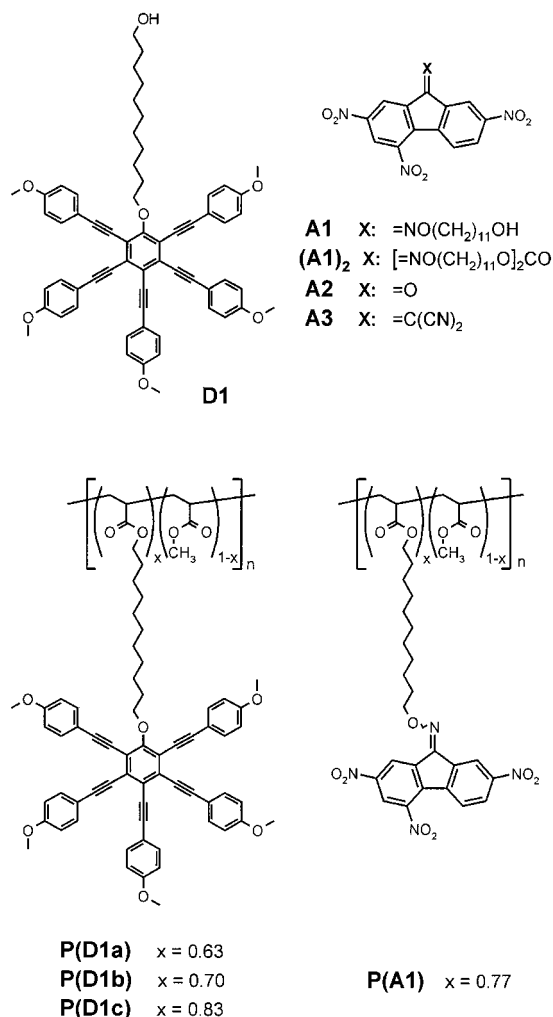


**Figure 3.** Studied materials.

below the glass temperature or obtained permanently by cross-linking the polymer in the mesophase. In the literature, these various aspects have been discussed by several contributions on discotic liquid crystalline main-chain<sup>5,9a-d</sup> and side-chain polymers<sup>5,9d-h</sup> as well as polymer networks.<sup>9h-j</sup>

Also, specific intra- and intermolecular interactions, like ionic, H-bond, and charge transfer (CT) interactions, play a crucial role in the phase formation of liquid crystals. Discotic mesogens have proven to be very suitable for CT complexation.<sup>10</sup> Because of their extended aromatic core, they can act as electron-rich "donors" when complexed with flat electron-deficient molecules. The electron acceptor 2,4,7-trinitro-9-fluorenone (TNF) or its derivatives are generally used, but other nitro-, cyano-, or fluoro-substituted arenes have also been investigated.<sup>10a,11</sup> Because of CT interactions, mesophases can be stabilized (extension of the temperature window of the mesophase), modified (another mesophase appears), or even induced (when complexing two non-liquid crystalline compounds).

Here, we report the liquid crystalline properties of the discotic mesogen **D1** (see Figure 3). By a straightforward polymer substitution reaction, the corresponding comb-shaped polymers, **P(D1)**, were prepared, and their liquid crystalline properties are compared to that of the low molar mass compound **D1**. The supramolecular CT complexes of **D1** with a series of non-liquid crystalline acceptors **A1**–**A3**, **(A1)<sub>2</sub>**, and **P(A1)** have been prepared.

The rich phase behavior of these complexes is presented, and it is clearly demonstrated that the use of CT interactions offers a simple as well as versatile approach to obtain a broad variety of liquid crystalline phases.

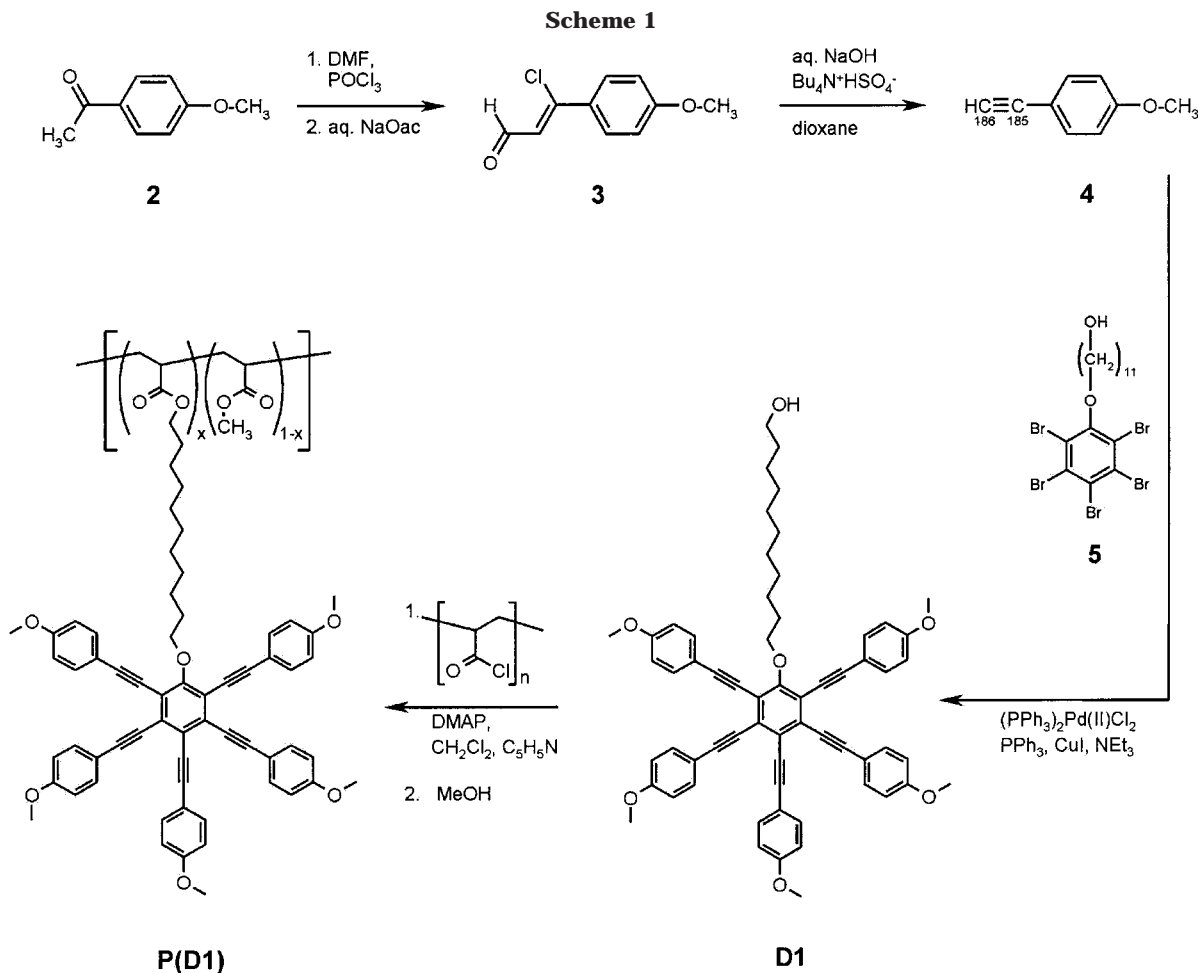
## Experimental Section

**Materials.** All materials were used as purchased unless mentioned otherwise. Pyridine was distilled from CaH<sub>2</sub> and CH<sub>2</sub>Cl<sub>2</sub> from P<sub>2</sub>O<sub>5</sub>. The synthesis of acceptors **A1**, **A2**, and **P(A1)** was described earlier.<sup>12</sup> Acceptor **A3** is commercially available. Pentabromophenol derivative<sup>13</sup> **5** and poly(acryloyl chloride)<sup>8a,b</sup> were prepared according to literature procedures. A crude solution of poly(acryloyl chloride) ( $M_n = 3000 \text{ g mol}^{-1}$ , PDI = 2.9) was stored in a refrigerator and used without further purification.

**Instrumentation.** Nuclear magnetic resonance (NMR) spectra were recorded on a Varian VXR 300 or VXR 400 MHz spectrometer. Chemical shifts are reported in ppm relative to tetramethylsilane. Molecular weights were determined by gel permeation chromatography (GPC) in THF against narrow polystyrene standards. Thermal properties of the materials were investigated using a Perkin-Elmer DSC 7 differential scanning calorimeter (in nitrogen atmosphere) and a Jenapol optical polarizing microscope, equipped with a Mettler FP82 HT hot stage and a Mettler FP80 central processor. The extent of order in the mesophases was studied with X-ray diffraction analysis, using a Siemens Kristalloflex 710D X-ray generator with graphite monochromated Cu K $\alpha$  radiation ( $\lambda = 1.54 \text{ \AA}$ ), equipped with a Bruker HI-STAR area detector. Samples were oriented in a magnetic field using a Supper SmCo permanent magnet with a field of about 1.5 T and heated using a custom-built capillary heating element.

**4-Ethynylanisole (4).** Phosphorus oxychloride (50 mL) was added dropwise to DMF (200 mL) at 0 °C. The mixture was allowed to warm to room temperature, stirred for 30 min, and cooled to 0 °C, and a solution of **2** (25 g, 167 mmol) in DMF (50 mL) was added in 15 min. After addition, the mixture was heated at 50 °C until TLC indicated complete consumption of the starting material. The reaction mixture was poured into a 20% sodium acetate solution (1 L), allowing the mixture to heat to 60 °C. After cooling overnight, the crude intermediate product **3** was filtered from the solution in a ~90% yield. The yellow solid was used for the next reaction without further purification. A small sample was crystallized from ethanol for NMR analysis. <sup>1</sup>H NMR (CDCl<sub>3</sub>):  $\delta$  10.12 (d, 1H, CHO); 7.88, 7.12 (2  $\times$  dd, 2  $\times$  2H, CH aromatic); 6.77 (d, 1H, C=CH); 3.92 (s, 3H, CH<sub>3</sub>O). A solution of **3** (all from the previous steps) and the phase transfer catalyst tetrabutylammonium hydrogen sulfate (0.5 g, 1.5 mmol) in dioxane (200 mL) was refluxed, and a 2 N NaOH solution (250 mL) was added at once. The dark solution was refluxed for 30 min, cooled, and neutralized, and the dioxane was evaporated under reduced pressure. The aqueous layer was extracted with diethyl ether (3 $\times$ ), and the combined organic layers were washed with a 1 N HCl solution (2 $\times$ ), water (2 $\times$ ) and brine (1 $\times$ ) and dried on MgSO<sub>4</sub>, and the solvent was evaporated. Pure **4** was obtained by highly concentrated separation over a column. The crude product was diluted with 40 mL eluent (CH<sub>2</sub>Cl<sub>2</sub>:hexane 1:2) and applied to a 300 mL column of SiO<sub>2</sub>. Extraction with the eluent, until all product was regained, yielded a colorless oil in 70% (overall yield). <sup>1</sup>H NMR (CDCl<sub>3</sub>):  $\delta$  7.41, 6.82, (2  $\times$  dd, 2  $\times$  2H, CH aromatic); 3.77 (s, 3H, CH<sub>3</sub>O); 2.98 (s, 1H, C $\equiv$ CH).

**11-[Pentakis(4-methoxyphenylethynyl)phenoxy]undecan-1-ol (D1).** A mixture of **4** (6.6 g, 50 mmol), **5** (3.3 g, 5.0 mmol), Pd(II)Cl<sub>2</sub>(PPh<sub>3</sub>)<sub>2</sub> (300 mg, 0.43 mmol), and PPh<sub>3</sub> (250 mg, 0.95 mmol) in 50 mL of triethylamine was degassed and stirred in an inert atmosphere until the alcohol was dissolved. Copper(I) iodide (200 mg, 1.05 mmol) was dissolved in 5 mL of THF with anhydrous LiBr (1.0 g) and added to the reaction mixture. After 8 h stirring at 90 °C, the mixture was poured into a 2 N HCl solution (200 mL), and the product was extracted with CH<sub>2</sub>Cl<sub>2</sub>. The reaction product was purified by column chromatography (SiO<sub>2</sub>, eluent: CH<sub>2</sub>Cl<sub>2</sub>:petroleum ether 4:1) and repeated crystallization from methanol. Yield: 2.47



g, 54% of a pale yellow, highly fluorescent powder.  $^1\text{H}$  NMR ( $\text{CDCl}_3$ ):  $\delta$  6.90–6.86, 7.56–7.51 ( $2 \times m$ , 20H, CH aromatic); 4.37 (t, 2H,  $\text{CH}_2\text{OPh}$ ); 3.83 (s, 15H,  $\text{OCH}_3$ ); 3.61 (t, 2H,  $\text{CH}_2\text{-OH}$ ); 1.95–1.10 (m, 18H,  $\text{CH}_2$  spacer).  $^{13}\text{C}$  NMR ( $\text{CDCl}_3$ ):  $\delta$  160.0, 159.9 (outer phenyl C–O); 159.8 (inner phenyl C–O); 133.3, 133.1 (outer phenyl CH); 128.3, 123.8, 119.9 (inner phenyl); 115.8, 115.6, 115.5 (outer phenyl, attached to acetylene); 114.1 (outer phenyl, CH); 99.2, 99.0, 97.0 (inner ethynyl); 88.7, 86.2, 83.6 (outer ethynyl); 74.6 ( $\text{CH}_2\text{OPh}$ ); 63.1 ( $\text{CH}_2\text{OH}$ ); 55.3 ( $\text{CH}_3\text{O}$ ); 32.8, 30.6, 29.6, 29.4, 26.4, 25.8 ( $\text{CH}_2$  spacer).

**Poly[11-(pentakis(4-methoxyphenylethynyl)phenoxy)-undecyl acrylate-co-methyl acrylate] P(D1).** The polymer analogous reaction has been described in detail elsewhere.<sup>7a,b</sup> Three different batches were prepared, starting from a slightly different mesogen–poly(acryloyl chloride) ratio. To remove nonreacted mesogen, the polymer was precipitated in methanol ( $2 \times$ ) and acetone ( $2 \times$ ). The degree of substitution, as calculated from peak intensities of the  $^1\text{H}$  NMR spectrum, was found to be 63%, 70%, and 83%. Yields were between 50 and 71% based on mesogen conversion. All peaks broadened significantly, so that no peak splitting was detected.  $^1\text{H}$  NMR ( $\text{CDCl}_3$ ):  $\delta$  7.6–7.2 (CH aromatic); 4.0 ( $\text{CH}_2\text{OPh}$ ); 4.3 ( $\text{CO}_2\text{CH}_2$ ); 3.6 ( $\text{CH}_3$  methyl acrylate); 2.5–1.1 ( $\text{CH}_2$ , CH aliphatic spacer and backbone).

**Carboxylic Acid Bis[11-(2,4,7-trinitrofluoren-9-ylidene-aminoxy)undecyl] ester (A1)<sub>2</sub>.** To a solution of **A1** (1.70 g, 2.14 mmol) and pyridine (180 mg, 2.14 mmol) in  $\text{CH}_2\text{Cl}_2$  (10 mL) was added diphosgene (182 mg, 0.9 mmol) via a syringe. The mixture was stirred for 12 h at room temperature, diluted with  $\text{CH}_2\text{Cl}_2$ , and washed with water. Pure (**A1**)<sub>2</sub> was obtained after purification by column chromatography ( $\text{SiO}_2$ , eluent: toluene:petroleum ether 40–60 1:1) as a pale yellow powder in a 54% yield.  $T_m = 71$ – $88$  °C due to the presence of *E/Z* isomers.  $^1\text{H}$  NMR ( $\text{CDCl}_3$ ):  $\delta$  9.46–8.21 (m of *E/Z* isomers, 10H, CH fluorene); 4.63 (t, 4H,  $\text{CH}_2\text{ON}$ ); 3.52 (t, 4H,  $\text{CH}_2\text{OCO}$ ); 1.96–1.28 (m, 36H,  $\text{CH}_2$  spacer).

**Charge Transfer Complexes.** Charge transfer (CT) complexes were prepared by dissolving the appropriate amounts of donor and acceptor in a common solvent ( $\text{CH}_2\text{Cl}_2$  or  $\text{CHCl}_3$ ). Evaporation of the solvent and drying for 24 h in vacuo yielded the complexes as strongly colored solids. Strangely, the thermal results of the CT complexes with **P(D1)** were hard to interpret, due to the weak and broad phase transitions and the slowly developing optical textures. For example, the complex **P(D1a):A1** was similar in phase behavior to the opposite complex **D1:P(A1)**, but the transitions in **D1:P(A1)** were much sharper and showed higher latent heat values. This is in contrast to what we observed before, for a series of other macromolecular charge transfer complexes.<sup>12</sup>

## Results and Discussion

**Synthesis.** The synthesis of **D1** and **P(D1)** is outlined in Scheme 1. The terminal acetylene **4** was prepared by a Vilsmeier–Haack reaction, followed by an elimination of a formic acid derivative under basic conditions.<sup>14</sup> In our laboratories, this method has been readily scaled up to the here-described quantities. Application of a phase transfer catalyst enabled us to use a much higher concentrated reaction mixture in the elimination step. Mesogen **D1** was prepared by a 5-fold palladium(0)-mediated cross-coupling reaction<sup>15</sup> between **4** and **5**, similar as described in the literature.<sup>8a</sup> Polymer **P(D1)** was prepared by a polymer analogous reaction, an esterification reaction between **D1** and the reactive poly(acryloyl chloride) under mild conditions. From  $^1\text{H}$  NMR analysis the various degrees of substitution were calculated, i.e., 63%, 70%, and 83% for **P(D1a)**, **P(D1b)**, and **P(D1c)**, respectively.

**Thermal Behavior.** The thermal behavior of the pure compounds was determined by optical polarizing

**Table 1. Thermal Behavior of D1-Based Liquid Crystals, Measured with OPM and DSC<sup>a</sup>**

D1	K	132 (37)	N <sub>D</sub>	246 (0.2)	I/d
P(D1a)	G <sub>N</sub>	41	N <sub>D</sub>	>200	d
P(D1b)	G <sub>N</sub>	50	N <sub>D</sub>	>200	d
P(D1c)	G <sub>N</sub>	45	N <sub>D</sub>	>200	d

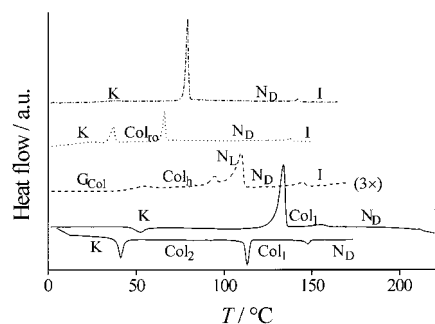
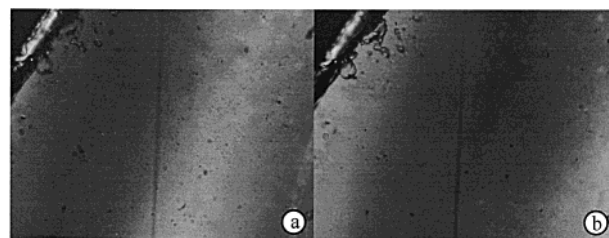
<sup>a</sup> Transition temperatures are shown in °C and latent heat values (in parentheses) in kJ mol<sup>-1</sup>. K = crystalline; G<sub>N</sub> = glassy (nematic phase frozen in); N<sub>D</sub> = nematic discotic; I = isotropic; d = decomposition. The exact clearing temperature is difficult to measure, since that material starts degrading at elevated temperatures.

microscopy (OPM) and differential scanning calorimetry (DSC). The results are summarized in Table 1.

Despite the absence of multiple long tails, **D1** showed a N<sub>D</sub> mesophase over a broad temperature range. Mesogens with the 5-fold (phenylethynyl)-substituted arene cores are known to display liquid crystalline behavior in the absence of multiple tails that are usually required for discotic liquid crystals. The mesogen with the methyl-substituted core that we investigated thoroughly before<sup>8,10c,16</sup> is another example of such behavior. The corresponding side-chain polymers **P(D1)** did not crystallize, but the N<sub>D</sub> mesophase froze in below the glass transition temperature. This resulted in materials with nematic discotic mesophases over a temperature range of more than 160 °C, which is unusually wide.<sup>17</sup> The observed glass transitions are close to each other, suggesting a rather independent behavior toward the degree of substitution, bearing in mind that only three polymers have been investigated. The acceptors did not show any liquid crystalline behavior; **A1–A3** and **(A1)<sub>2</sub>** are crystalline solids with melting temperatures of 98–109, 176, 276, and 71–88 °C, respectively,<sup>18</sup> and **P(A1)** is an amorphous polymer with a glass transition temperature of 50 °C.<sup>7a</sup>

**Charge Transfer Complexes.** OPM studies of donor–acceptor contact samples, combined with DSC of CT complexes at various molar ratios, were used to investigate the phase behavior of the complexes as a function of acceptor concentration. It appeared that at exact equimolar concentrations the best properties were found, i.e., the highest clearing temperature and no biphasic areas. This indicates that at such concentrations a stable complex is formed that effectively induces a single liquid crystalline CT species. This is similar to what was observed before in other CT complexes.<sup>6,7a,12</sup>

Combining the acceptors with **D1** induced several liquid crystalline phases (see Table 2). Interaction of acceptor **A1** reduced the melting point of **D1**, but even more the clearing temperature, which narrowed the temperature window of the mesophase substantially (Figure 4a). This is indicative of a strong destabilizing effect on the nematic mesophase. The analogous complex with the dimeric acceptor **D1:(A1)<sub>2</sub>** showed a N<sub>D</sub> phase at high temperatures and an additional columnar

**Figure 4.** DSC thermograms of (a) **D1:A1** (---), (b) **D1:(A2)<sub>2</sub>** (· · ·), (c) **D1:P(A1)** (- - -), and (d) **D1:A2** (—).**Figure 5.** Photographs of optical textures of uniform planar aligned nematic phase of (a) **D2:P(A1)** at 100 °C (N<sub>L</sub> phase) and (b) **D2:P(A1)** at 120 °C (N<sub>D</sub> phase). Both pictures were taken at exactly the same spot with crossed polarizers; magnification 45×.

phase, prior to crystallization at low temperatures (Figure 4b). The complex of **D1** with the corresponding **P(A1)** showed a similar behavior at high temperatures, i.e., a nematic phase and a reduced clearing temperature. At lower temperatures crystallization was suppressed, which resulted in a pronounced polymorphism, clearly shown by the DSC thermogram (Figure 4c). Cooling down from the isotropic phase, first the N<sub>D</sub> phase was observed. The optical texture (Figure 5) did not change at the transition to the recently reported N<sub>L</sub> phase.<sup>7b,c</sup> Upon further cooling a transition to a columnar hexagonal phase was found, which could be identified by the optical texture after extensive annealing at 80 °C.

The role of acceptor strength was investigated by complexing **D1** with acceptors of increasing electron deficiencies. The acceptor strength is determined as **A1** ≈ **(A1)<sub>2</sub>** ≈ **P(A1)** < **A2** < **A3**. Compared with **D1:A1**, discussed above, the N<sub>D</sub> phase of **D1:A2** occurred at higher temperatures. The heating curve of the thermogram (Figure 4) showed a columnar phase (Col<sub>1</sub>) between the crystalline and the nematic discotic phase. Because of supercooling of the crystalline phase, a second columnar phase (Col<sub>2</sub>) was revealed in the cooling run. Both phases were easily recognized as columnar phases by their characteristic optical textures, shown in Figure 6. The Col<sub>2</sub> phase is metastable, since annealing at 100 °C for hours did not cause crystallization.

**Table 2. Thermal Behavior of Equimolar Complexes of CT Complexes with D1 and Various Acceptors, Measured with OPM and DSC<sup>a</sup>**

complex D1 with											
<b>A1</b>	K	80 (16)						N <sub>D</sub>	146 (0.5)	I	
<b>(A1)<sub>2</sub></b>	K	37 (4.6)						N <sub>D</sub>	137 (0.6)	I	
<b>P(A1)</b>	G <sub>Col</sub>	45	Col <sub>h</sub>	94 (2.0)	N <sub>L</sub>	110 (7.5)		N <sub>D</sub>	146 (0.5)	I	
<b>A2</b>	K	[41 (7.6)	Col <sub>2</sub>	110 (6.1)] <sup>b</sup>	134 (53)	Col <sub>1</sub>	150 (2.0)		N <sub>D</sub>	216 (0.8)	I
<b>A3</b>	G <sub>Col</sub>	18	Col <sub>ro</sub>	148 (6.0)	Col <sub>hd</sub>				220–230	I/d	

<sup>a</sup> Transition temperatures are shown in °C and latent heat values (between the brackets) in kJ mol<sup>-1</sup>. K = crystalline; G<sub>M/Col</sub> = glassy (mesophase/columnar phase frozen in); N<sub>D</sub> = nematic discotic; N<sub>L</sub> = nematic lateral; Col<sub>ho</sub> = columnar hexagonal, ordered; Col<sub>hd</sub> = columnar hexagonal, disordered; Col<sub>ro</sub> = columnar rectangular, ordered; I = isotropic; d = decomposition. <sup>b</sup> Monotropic phase transition.

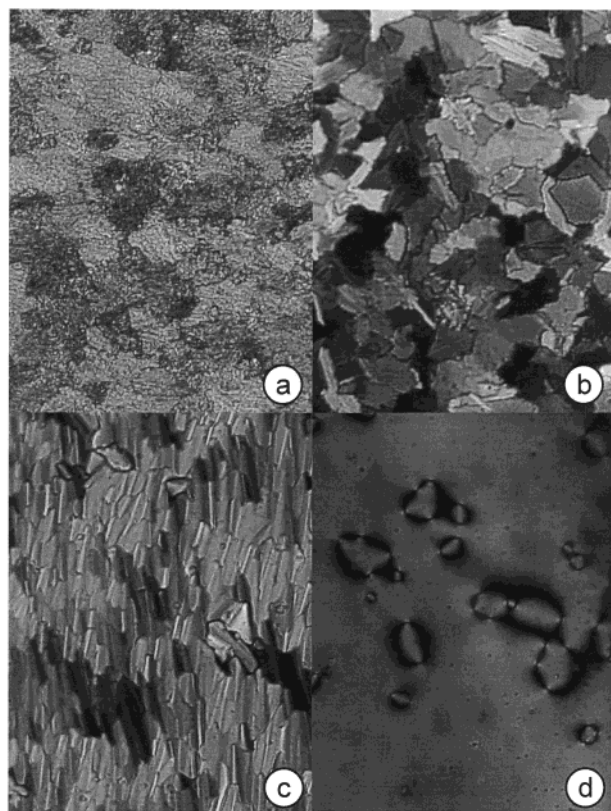


**Figure 6.** Photographs of optical textures of **D1:A2** at (a) 40 °C (grainy texture, crystalline phase), (b) 100 °C (mosaic texture,  $\text{Col}_2$  phase), (c) 130 °C ( $\text{Col}_1$  phase), and (d) 160 °C (schlieren texture,  $\text{N}_D$  phase). All pictures were taken with crossed polarizers; magnification 167 $\times$ .

In the complex with the stronger acceptor **D1:A3**, the nematic discotic phase was completely replaced by a columnar phase, also at high temperatures. Upon cooling, a transition into a columnar phase was observed, showing a highly viscous texture that developed very slowly. At lower temperatures a second-order transition was found, where the liquid crystalline phase was frozen in. This is similar to what was observed in derivatives of triphenylenes<sup>19</sup> and CT complexes of substituted triphenylenes with **A2**.<sup>20</sup> In these studies, the second-order transition was attributed to a transition into a columnar plastic phase, which is characterized by a three-dimensional positional order of the molecules, while the molecules keep their rotational mobility, analogous to the soft crystal B phase in rod-shaped liquid crystals. The thermal results of the CT complexes of **D1** are summarized in Table 2.

**Powder X-ray Reflection Measurements.** Temperature-dependent X-ray diffraction (XRD) measurements were performed on **D1** and its corresponding side chain polymers as well as on the charge transfer complexes of **D1** with the electron acceptors. The spacings  $d$  were calculated, using the Bragg law  $2d \sin(\theta) = n\lambda$ , where  $\theta$  is the diffraction angle,  $n$  is an integer, and  $\lambda$  is the wavelength (1.54 Å). For a more quantitative analysis on the extent of order in the materials, the correlation length  $\xi$ , which is a measure for the length scale of positional order, was calculated using

$$\xi = \frac{0.89\lambda}{\omega_{1/2} \cos(\theta_0)} \quad (1)$$

Here,  $\omega_{1/2}$  is the full width at half-maximum of the

**Table 3. XRD Results D1-based Mesogens**

discotic mesogen	$T$ [°C]	phase <sup>a</sup>	lateral direction		"columnar" direction	
			$d_{100}$ [Å]	$\xi_{100}$ [Å]	$d_{001}$ [Å]	$\xi_{001}$ [Å]
<b>D1</b>	160	$\text{N}_D$	15.2	22	4.02	11
<b>P(D1b)</b>	50	$\text{N}_D$	15.0	29	4.12	13
<b>P(D1b)</b>	150	$\text{N}_D$	15.2	23	4.25	13
<b>P(D1c)</b>	50	$\text{N}_D$	14.5	23	4.09	9
<b>P(D1c)</b>	150	$\text{N}_D$	14.8	22	4.19	8

<sup>a</sup> Phases:  $\text{N}_D$  = nematic discotic.

**Table 4. XRD Results of High and Low Molar Mass CT Complexes**

CT complex	$T$ [°C]	phase <sup>a</sup>	$d_{200}$ [Å]	$\xi_{200}$ [Å]	$d_{001}$ [Å]	$\xi_{001}$ [Å]
<b>D1:A1</b>	130	$\text{N}_D$	15.5	25	3.6	19
<b>D1:(A1)<sub>2</sub></b>	50	$\text{Col}_{ro}^b$	16.2	126	3.6	80
	100	$\text{N}_D$	16.3	41	3.8	13
<b>D1:P(A1)</b>	80	$\text{Col}_{ho}^d$	13.6	206	3.5	87
	100	$\text{N}_L$	13.7	148	3.6	43
	130	$\text{N}_D$	14.3	36	3.7	16
<b>D1:A2</b>	105	$\text{Col}_2^d$	15.7	33	3.5	16
	130	$\text{Col}_1^d$	15.6	31	3.6	12
	160	$\text{N}_D$	15.5	28	3.7	11
<b>D1:A3</b>	130	$\text{Col}_{ro}^c$	15.3	120	3.6	68
	160	$\text{Col}_{hd}^d$	14.2	117	3.6	32

<sup>a</sup> Phases:  $\text{N}_D$  = nematic discotic;  $\text{N}_L$  = nematic lamellar;  $\text{Col}_{ro}$  = columnar rectangular ordered;  $\text{Col}_{ho}$  = columnar hexagonal ordered;  $\text{Col}_{hd}$  = columnar hexagonal disordered. <sup>b</sup> Rectangular phase:  $d_{010} = 11.8$  Å ( $\xi_{010} = 74$  Å) with lattice parameters  $a = 33.1$ ,  $b = 23.4$ ,  $\alpha = 45^\circ$ . <sup>c</sup> Rectangular phase:  $d_{010} = 11.1$  Å ( $\xi_{010} = 83$  Å) with lattice parameters  $a = 31.0$ ,  $b = 21.9$ ,  $\alpha = 45^\circ$ . <sup>d</sup> The lattice parameters of the hexagonal columnar phases can be calculated from the intercolumnar spacing:  $a = b = 4d_{200}/\sqrt{3}$  and  $\alpha = 60^\circ$ .

reflection, and the diffraction angle  $\theta_0$  is the maximum of the reflection. Both are easily determined after fitting the X-ray patterns with Lorentzian profiles.

Powder XRD patterns of the nematic phases of **D1** and polymers **P(D1)** were nearly identical. They all showed very diffuse reflections, and the samples hardly aligned in the  $\sim 1.5$  T magnetic field around the sample holder. The low order of the  $\text{N}_D$  phase is clearly demonstrated by the low correlation lengths in the both lateral  $[hk0]$  and the columnar  $[00l]$  direction,<sup>21</sup> as shown in Table 3. These correlation lengths were among the lowest that we have measured in our laboratories, compared to X-ray data of  $\text{N}_D$  phases of other disk-shaped mesogens. Upon heating **D1** slightly above the clearing temperature, the correlation lengths hardly changed. Polymers **P(D1a–c)** show a very broad nematic phase. XRD measurements were performed from 30 to 190 °C to study the temperature dependence of the molecular spacings  $d$  and correlation lengths  $\xi$  in the nematic discotic phase. With increasing temperature, an expected slight increase in the lateral and "columnar" spacings was observed, combined with a small decrease in the corresponding correlation lengths. Unfortunately, because of the broad, diffuse reflections (low order) which are hard to fit, no quantify data could be obtained. Furthermore, no differences between the polymers with an increasing degree of substitution could be observed.

Because of the CT interactions in the  $\text{N}_D$  phase of **D1:A1**, the correlation lengths increased slightly, especially in the columnar  $[001]$  direction (see Table 4). However, the mesophase still was characterized as  $\text{N}_D$ . Both the analogous dimer complex **D1:(A1)<sub>2</sub>** and macromolecular complex **D1:P(A1)** showed equivalent XRD patterns of

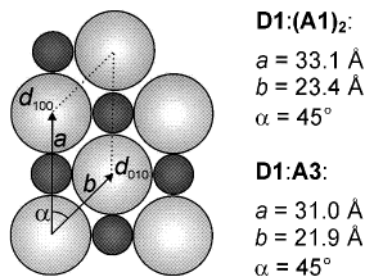


**Figure 7.** Schematic representation of the columnar rectangular phase of **D1:P(A1)** and **D1:A3**. Note that the donors (light) have about twice the diameter of the acceptors (dark).

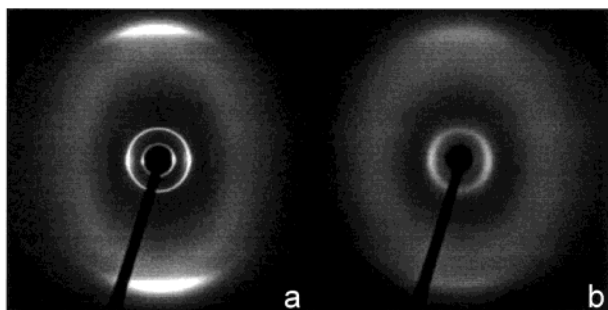


**Figure 8.** XRD patterns of CT complex **D1:P(A1)** at (a) 100 °C ( $N_L$  phase) and (b) 130 °C ( $N_D$  phase). Maximum diffraction angle:  $2\theta = 30^\circ$ .

the  $N_D$  phase. At lower temperatures, **D1:(A1)<sub>2</sub>** underwent a transition to a columnar rectangular ( $Col_{rd}$ ) phase, which was characterized by only two reflections, attributed to the  $d_{200}$  and  $d_{010}$  spacings. By estimating the volume of a unit cell (using a density of  $1.05 \text{ kg dm}^{-3}$ ) from the molecular mass of the complex, we were able to calculate approximate values of the lattice parameters  $a$ ,  $b$  and the angle  $\alpha$ ,<sup>22</sup> as presented in Figure 7. Upon cooling **D1:P(A1)** from the  $N_D$  phase (Figure 8b) into the  $N_L$  phase (Figure 8a), the complex aligned in the 1.5 T magnetic field. Both the [200] and the [001] reflections sharpened considerably, and an additional reflection, attributed to the [100] reflection, was observed at small angles.<sup>7a</sup> The difference in order between the two nematic phases is most clearly shown in the radial scans, shown in Figure 10a. By cooling the sample into the columnar phase, further increase of the correlation lengths in both the columnar and lateral direction was observed. It is stressed that it is difficult to make an unambiguous statement of the type of columnar mesophase, because XRD measurements only show two reflections and the OPM experiments showed a highly viscous texture that developed slowly. To confirm the  $Col_h$  phase, XRD patterns must be recorded parallel to the columns of a macroscopically aligned sample. However, as yet we have not succeeded in preparing such samples.

Charge transfer complexes of **D1:A2** display a very interesting set of XRD results (see Figures 9 and 10b). At high temperatures, **D1:A2** showed a  $N_D$  phase, easily identified by its diffuse diffraction pattern (Figure 9d) and, of course, supported by the clear *schlieren* texture, observed in OPM experiments. Upon cooling from the  $N_D$  phase, a transition into an intermediately viscous mesophase is observed. This mesophase shows the typical features of a columnar phase, i.e., the characteristic optical texture (Figure 6c) and a  $1.2 \text{ kJ mol}^{-1}$  latent heat upon formation of the phase. However, XRD experiments showed different results (Figure 9c). The

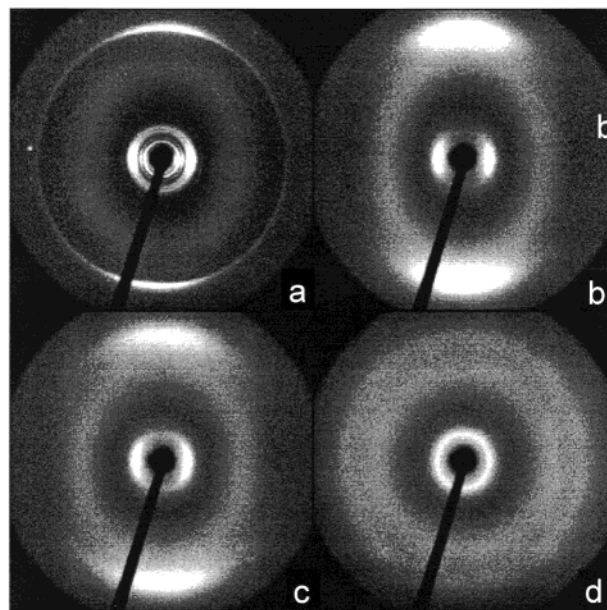


**Figure 9.** XRD patterns of CT complex **D1:A2** at (a) 40 °C ( $K$  phase), (b) 105 °C ( $Col_2$  phase, obtained by cooling from the  $Col_1$  phase), (c) 130 °C ( $Col_1$  phase), and (d) 160 °C ( $N_D$  phase). Maximum diffraction angle:  $2\theta = 30^\circ$ .

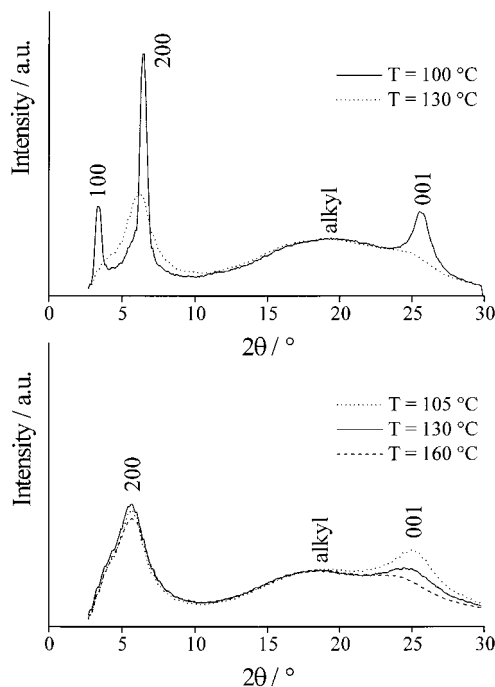


**Figure 10.** XRD diagrams of (a) **D1:P(A1)** at 100 °C ( $N_L$  phase) and 130 °C ( $N_D$  phase) and (b) **D1:A2** at 105 °C ( $Col_2$  phase), 130 °C ( $Col_1$  phase), and 160 °C ( $N_D$  phase).

pattern is weakly aligned in the magnetic field, and the radially integrated pattern (Figure 10b) is still very diffuse. The intercolumnar reflection ( $d_{200}$ ), which is usually well-developed in a columnar phase, is identical to the reflection observed for the  $N_D$  phase at 160 °C. The [001] reflection shows only a minor increase of the intracolumnar order. These results strongly oppose any suggestion of long-range positional order in the mesophase, which is indicated beyond any doubt by the optical texture. Note that the low correlation lengths are a marked contrast to correlation lengths of columnar phases of CT complexes that have been reported in the literature, where columnar phases with correlation

lengths as high as 200 Å in the lateral direction and 50 Å in the columnar direction are reported.<sup>24</sup> An imaginable phase assignment<sup>25a</sup> could be a Col<sub>hd</sub> phase: hexagonal since only one reflection is observed in the small angle area and disordered because of the profound low order in the intracolumnar direction.

Before the sample crystallized at low temperatures (the crystalline pattern with many sharp reflections in the small angle region is shown in Figure 9a), another mesophase appeared, showing an increased viscosity, and an optical mosaic-like texture (Figure 6b), characteristic of a columnar phases. Peculiarly, again, the XRD pattern (Figure 9b) remained very diffuse. In the intercolumnar direction, the radially integrated pattern (Figure 10b) is still identical to that of the first columnar phase and the N<sub>D</sub> phase. In the intracolumnar direction, a slight increase in order is observed with respect to the first columnar phase. Now, interpretation of the XRD results is even harder. The unchanged reflection in the small angle region indicates the preservation of a hexagonal arrangement.<sup>25b</sup> Taking the small sharpening of the intracolumnar reflection into account leads to the assignment of a Col<sub>ho</sub> phase for the second columnar phase. However, the assignment to a Col<sub>ho</sub> and the subsequent transition to a Col<sub>hd</sub> phase is in contradiction with the Landau–Peierls instability criterion, which predicts that one-dimensional true long-range order, and therefore a transition from the Col<sub>hd</sub> to the Col<sub>ho</sub> phase, is prohibited.<sup>26</sup>

XRD experiments on the complex **D1:A3** showed the anticipated behavior. The characteristic patterns of well-ordered columnar phases were observed. The Col<sub>hd</sub> phase shows only one sharp intercolumnar reflection. In the Col<sub>ro</sub> phase a second reflection in the small angle region appeared that defines the rectangular lattice. At the transition from the Col<sub>ro</sub> phase to the Col<sub>hd</sub> phase, the correlation length in the lateral direction ( $\xi_{200}$ ) remains constant. The correlation length in the columnar direction ( $\xi_{001}$ ) decreases suddenly, indicating a strong loss of order within the columns.

**Birefringence Studies.** Because complex **D1:P(A1)** shows one of the first examples of a nematic–nematic phase transition, we decided to investigate the nature of the transition more closely. The relative optical retardation ( $\Delta\Gamma/T$ ) was measured in a polarizing microscope using a variable compensator. The optical retardation is linearly correlated to the birefringence:  $\Gamma \propto d\Delta n$ , where  $d$  is the (constant) sample thickness. The results were plotted and fitted to an extended Maier–Saupe curve,<sup>27</sup> showing the temperature dependence of the order parameter  $\langle P_2 \rangle$ , using eq 2.

$$\Gamma \propto c_1 \langle P_2 \rangle \quad (2a)$$

$$\langle P_2 \rangle = 0.1 + 0.9 \left\{ 1 - 0.99 \left( \frac{T}{T_N} \right)^{c_2} \right\}^{1/4} \quad (2b)$$

Nematic phases can be described satisfactory with an (extended) Maier–Saupe curve. Therefore, eq 2 was used to fit both the N<sub>L</sub> phase and the N<sub>D</sub> phase. In eq 2, the fitting parameter  $T_N$  represents the transition temperature of the N<sub>L</sub> to N<sub>D</sub> transition or the N<sub>D</sub> to I transition, respectively.<sup>28a</sup> Constants  $c_1$  and  $c_2$  are fitting parameters as well. Note that  $c_1$  is used to fix the  $y$ -axis at  $\langle P_2 \rangle = 1$  for  $T = 0$  K, which is required by the definition of  $\langle P_2 \rangle$ . Constant  $c_2$  equals 1 for the common Maier–Saupe model, but larger values have been found

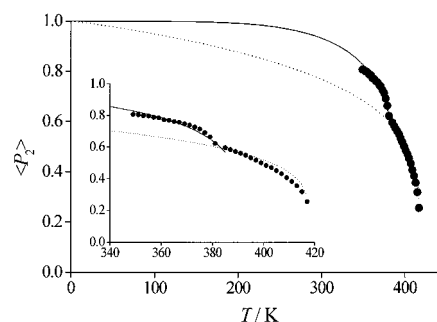


**Figure 11.** Temperature dependence of the order parameter: (●) experimental data; (—) and (· · ·) fits of the N<sub>L</sub> phase and N<sub>D</sub> phase using eq 3. The inset shows a magnification.

for polymer materials (here, in the N<sub>D</sub> phase  $c_2 = 1$  and in the N<sub>L</sub> phase  $c_2 = 2$ ).<sup>28b</sup> The thermal dependence of the order parameter  $\langle P_2 \rangle$  is shown in Figure 11.

The fits are in good agreement with the experimental data. At the crystal–nematic phase transition a strong inflection point is observed. However, for a first-order phase transition, a discontinuity of the order parameter at the phase transition is expected, which was not observed.

## Conclusions

We have prepared a series of CT complexes of the nematogenic donor **D1** and the non-liquid crystalline acceptors **A1–A3** (low molar mass), (**A1**)<sub>2</sub> (dimer), and **P(A1)** (polymer). A wide range of mesophases were observed for the CT complexes, ranging from a destabilized N<sub>D</sub> phase for the **D1:A1** complex to a well-ordered Col<sub>ho</sub> phase of the **D1:A3** complex. Application of the same acceptor moiety in the form of a “monomer”, dimer, or polymer has a large impact on the phase behavior. All three CT complexes show a N<sub>D</sub> phase at high temperatures, however, where **D1:A1** crystallizes **D1:(A1)<sub>2</sub>** and **D1:P(A1)** showed transitions to higher ordered columnar phases. In addition, the macromolecular complex showed the recently identified N<sub>L</sub> phase. A remarkable behavior was observed for complex **D1:A2** that clearly showed two columnar phases during OPM experiments, whereas XRD experiments showed only diffuse reflections.

It is established that X-ray diffraction is a very useful tool to investigate the order in liquid crystalline phases. However, one has to be conscious of the fact that X-rays mainly probe the *local* environment of an average mesogen or supramolecular assembly of mesogens. From the results based on XRD experiments, conclusions can only be drawn concerning length scales that are of the same order of the measured spacings. Commonly, this is the case, and XRD provides an excellent tool to establish the order in mesophases. However, for more complex systems, like presented in this contribution, misinterpretations can be easily made. For example, the N<sub>L</sub> phase of **D1:P(A1)** has a XRD pattern of a common columnar phase but shows all the other features of a nematic phase. On the other hand, the Col<sub>1</sub> and Col<sub>2</sub> phase of complex **D1:A2** show a XRD pattern typical for a nematic phase, but both show the optical characteristics of a columnar phase. The latter result seems to imply that it is possible to have columnar phases where the packing of the columns remains rather disordered. These materials should therefore be considered as possible “amorphous columnar phases (Col<sub>A</sub> phases)”, which can be subdivided into Col<sub>A0</sub> and Col<sub>Ad</sub> phases, dependent on the intracolumnar order. In conclusion,

it clearly will be difficult to distinguish the Col<sub>A</sub> phase from the well-established N<sub>Col</sub> phase, except by optical microscopy experiments and investigations of the local dynamics, e.g., by dielectric relaxation spectroscopy.

**Acknowledgment.** We thank Vanina Kleiman for the preparation of **D1** and Otto van den Berg for the preparation of the acceptors **A1**, **(A1)<sub>2</sub>**, and **P(A1)**. Ben Norder is acknowledged for technical assistance with the thermal analysis and Enno Klop of the Akzo Nobel Chemical Research Arnhem, Department of Applied Physics, for assistance in performing XRD analysis.

## References and Notes

- (1) Chandrasekhar, S.; Sadashiva, B. K.; Suresh, K. A. *Pramana* **1977**, *9*, 471.
- (2) For a review on discotic liquid crystals, read: (a) Cammidge, A. N.; Bushby, R. J. In *Handbook of Liquid Crystals*; Demus, D., Goodby, J. W., Gray, G. W., Spiess, H. W., Vill, V., Eds.; Wiley VCH: New York, 1998; Vol. 2B, pp 693–748. (b) Chandrasekhar, S. In *Handbook of Liquid Crystals*; Demus, D., Goodby, J. W., Gray, G. W., Spiess, H. W., Vill, V., Eds.; Wiley VCH: New York, 1998; Vol. 2B, pp 749–780 and references in both chapters.
- (3) Applications of discotic liquid crystals: (a) Kamada, K.; Watanabe, J.; Arakawa, K.; Kozono, H. Fuji Photo Film Co., Ltd. Eur. Pat. Appl. EP 646829 A1, 1995. (b) Mori, H.; Itoh, Y.; Nishiura, Y.; Nakamura, T.; Shinagawa, Y. *Jpn. J. Appl. Phys.* **1997**, *36*, 143–147. (c) Adam, D.; Schuhmacher, P.; Simmerer, J.; Haussling, L.; Siemensmeyer, K.; Etzbach, K. H.; Ringsdorf, H.; Haarer, D. *Nature (London)* **1994**, *371*, 141–143. (d) Boden, N.; Movaghar, B. In *Handbook of Liquid Crystals*; Demus, D., Goodby, J. W., Gray, G. W., Spiess, H. W., Vill, V., Eds.; Wiley VCH: New York, 1998; Vol. 2B, pp 781–798 and references therein.
- (4) Tinh, N. H.; Destrade, C.; Gasparoux, H. *Phys. Lett.* **1979**, *72A*, 25.
- (5) Ringsdorf, H.; Wüstefeld, R.; Zerta, E.; Ebert, M.; Wendorff, J. H. *Angew. Chem., Int. Ed. Engl.* **1989**, *28*, 914–918.
- (6) Praefcke, K.; Singer, D.; Kohne, B.; Ebert, M.; Liebmann, A.; Wendorff, J. H. *Liq. Cryst.* **1991**, *10*, 147–159.
- (7) (a) Kouwer, P. H. J.; Jager, W. F.; Mijs, W. J.; Picken, S. J. *Macromolecules* **2001**, *34*, 7582–7584. (b) A comprehensive discussion on the N<sub>L</sub> phase is given in ref 7a. For the sake of clarity, we give here some further experimental characteristics of the N<sub>L</sub> phase. The N<sub>L</sub> phase showed all the features required to unambiguously identify it as a nematic mesophase, even after extensive annealing. For example, a clear *schlieren* texture with  $\pm 1/2$  and  $\pm 1$  disclinations, occasional disclination lines, and a smooth appearance were observed in microscopy experiments. Long-range smectic or columnar order is not compatible with a *schlieren* texture due to the incompressibility of the lamellae or two-dimensional stacks. Defects in these materials result in typical focal conical textures (for lamellae) and “oak-leaf” or mosaic textures (for columns). A SmC phase, also exhibiting a *schlieren* texture in a homeotropic alignment, can be excluded due to the presence of clear  $\pm 1/2$  disclinations in our texture. Moreover, after deformation, the *schlieren* texture reappeared quickly. (c) If we would have been looking at a mesophase with long-range positional order, like a columnar phase, it would certainly have led to the formation of an (physically bonded) elastic network due to the presence of the polymer backbone, which is in strong contrast to the low viscosity that we observed in the material.
- (8) (a) Kouwer, P. H. J.; Mijs, W. J.; Jager, W. F.; Picken, S. J. *Macromolecules* **2000**, *33*, 4336–4342. (b) Kouwer, P. H. J.; Gast, J.; Jager, W. F.; Mijs, W. J.; Picken, S. J. *Mol. Cryst. Liq. Cryst.* **2001**, *364*, 225–234. (c) Kouwer, P. H. J.; Mijs, W. J.; Jager, W. F.; Picken, S. J. *J. Am. Chem. Soc.* **2001**, *123*, 4645–4646.
- (9) (a) Boden, N.; Bushby, R. J.; Cammidge, A. N.; Headdock, G. *J. Mater. Chem.* **1995**, *5*, 2275–2281. (b) Wenz, G. *Makrom. Chem., Rapid Commun.* **1985**, *6*, 577–584. (c) Herrmann-Schönherr, O.; Wendorff, J. H.; Kreuder, W.; Ringsdorf, H. *Makrom. Chem., Rapid Commun.* **1986**, *7*, 97–101. (d) Kreuder, W.; Ringsdorf, H. *Makrom. Chem., Rapid Commun.* **1983**, *4*, 807–815. (e) Boden, N.; Bushby, R. J.; Lu, Z. B. *Liq. Cryst.* **1998**, *25*, 47–58. (f) Weck, M.; Mohr, B.; Maughon, B. R.; Grubbs, R. H. *Macromolecules* **1997**, *30*, 6430–6437. (g) Stewart, D.; McHattie, G. S.; Imrie, C. T. *J. Mater. Chem.* **1998**, *8*, 47–51. (h) Favre-Nicolin, C. D.; Lub, J. *Macromolecules* **1996**, *29*, 6143–6149. (i) Disch, S.; Finkelmann, H.; Ringsdorf, H.; Schuhmacher, P. *Macromolecules* **1995**, *28*, 2424–2428. (j) Braun, C. D.; Lub, J. *Liq. Cryst.* **1999**, *26*, 1501–1509.
- (10) (a) Praefcke, K.; Singer, D. In *Handbook of Liquid Crystals*; Demus, D., Goodby, J. W., Gray, G. W., Spiess, H. W., Vill, V., Eds.; Wiley VCH: New York, 1998; Vol. 2B, pp 945–967. (b) Ringsdorf, H.; Wüstefeld, R. *Philos. Trans. R. Soc. London* **1990**, *A330*, 95–108. (c) Praefcke, K.; Holbrey, J. D. *J. Inclusion Phenom.* **1996**, *24*, 19–41.
- (11) (a) Davidson, P.; Levelut, A. M.; Strzelecka, H.; Gionis, V. *J. Phys. (Paris)* **1983**, *44*, L-823. (b) Weck, M.; Dunn, A. R.; Matsumoto, K.; Coates, G. W.; Lobkovsky, E. B.; Grubbs, R. H. *Angew. Chem., Int. Ed.* **1999**, *38*, 2741–2745.
- (12) Kouwer, P. H. J.; Berg, O. v. d.; Jager, W. F.; Mijs, W. J.; Picken, S. J. *Macromolecules* **2002**, *35*, 2576–2582.
- (13) Janietz, D.; Praefcke, K.; Singer, D. *Liq. Cryst.* **1993**, *13*, 247–253.
- (14) Rosenblum, M.; Brawn, N.; Papenmeier, J.; Applebaum, M. *J. Organomet. Chem.* **1966**, *6*, 173–180.
- (15) (a) Sonogashira, K.; Tohda, Y.; Nagihara, N. *Tetrahedron Lett.* **1975**, 4467. (b) Brandsma, L.; Vasilevsky, S. F.; Verkuijsse, H. D. In *Applications of Transition Metal Catalysis in Organic Synthesis*; Springer-Verlag: Berlin, 1998; pp 198–225.
- (16) Janietz, D. *Chem. Commun.* **1996**, 713–714.
- (17) From a fast OPM measurement on a (slowly degrading) polymer sample, a clearing temperature of the order of 230 °C could be determined.
- (18) The broad melting temperatures of **A1** and **(A1)<sub>2</sub>** are due to the presence of *EZ*-isomers of **A1** and hence three isomers for **(A1)<sub>2</sub>**.
- (19) Glösen, B.; Kettner, A.; Wendorff, J. H. *Mol. Cryst. Liq. Cryst.* **1997**, *303*, 115–120.
- (20) Unpublished results from investigations in our own laboratories.
- (21) Qualitatively discussed XRD results use the terms lateral for the [h00] or [0k0] direction and columnar for the [001] direction. Also, when no columns are present, like in the nematic discotic (N<sub>D</sub>) phase.
- (22) Usually, two spacing are not sufficient to calculate the parameters of a monoclinic unit cell (three variables: *a*, *b*, and  $\alpha$ ). Estimation of the volume of the unit cell, assuming that it consists of one donor and one acceptor disk, offered us a third known quantity to calculate the lattice parameters *a*, *b*, and  $\alpha$ . For example, a unit cell consisting of 1 **D1** and  $1/2$  **(A1)<sub>2</sub>** has a unit cell mass of  $M = M_{D1} + 1/2 M_{(A1)2} = 1428$  g mol<sup>-1</sup> and a unit cell volume of  $V = M/(\rho N_A) = 2.1$  nm<sup>3</sup>. Fitting the spacings with a monoclinic cell with a fixed volume gives the presented results.
- (23) Kouwer, P. H. J.; Jager, W. F.; Berg, O. v. d.; Mijs, W. J.; Picken, S. J. *Polym. Mater. Sci. Eng.* **2001**, *85*, 303–304.
- (24) (a) Bengs, H.; Karthaus, O.; Ringsdorf, H.; Baehr, C.; Ebert, M.; Wendorff, J. H. *Liq. Cryst.* **1991**, *10*, 161–168. (b) Ebert, M.; Frick, G.; Baehr, C.; Wendorff, J. H.; Wüstefeld, R.; Ringsdorf, H. *Liq. Cryst.* **1992**, *11*, 293–309. (c) Möller, M.; Tsukruk, V. V.; Wendorff, J. H.; Bengs, H.; Ringsdorf, H. *Liq. Cryst.* **1992**, *12*, 17–36.
- (25) (a) Contact samples of the complex **D1:A2** with discotic liquid crystals with a well-known mesophase are difficult to prepare. The electron acceptor **A2** also complexes the other mesogen and hence gives rise of a range of different mesophases, dependent on the exact local composition. Despite the effort, no conclusions could be drawn from these experiments. (b) A change in symmetry of the columnar organization (like the formation of a Col<sub>l</sub> or Col<sub>ob</sub> phase) would have resulted in, at least, an observable change in the small-angle region of the XRD pattern. Tilting of the disks in the columns would have resulted in a rectangular or oblique columnar arrangement and in an increase in the *d*<sub>001</sub> spacing.
- (26) Fontes, E.; Heiney, P. A.; de Jeu, W. H. *Phys. Rev. Lett.* **1988**, *61*, 1202–1205.
- (27) (a) Maier, W.; Saupe, A. *Z. Naturforsch.* **1958**, *13A*, 564. (b) Maier, W.; Saupe, A. *Z. Naturforsch.* **1959**, *14A*, 882. (c) Maier, W.; Saupe, A. *Z. Naturforsch.* **1960**, *15A*, 287.
- (28) (a) Obviously, for the N<sub>D</sub> phase *T<sub>N</sub>* should coincide with the clearing temperature: *T<sub>N</sub>* = *T<sub>i</sub>* = 419 K. (b) The mean-field potential *U* of the extended Maier–Saupe theory is defined as  $U = -\epsilon(T)\langle P_2 \rangle P_2(\cos \theta)$ , where  $\epsilon(T) \propto T^{1-\epsilon_2}$ . A value of  $\epsilon_2 \neq 1$  corresponds to an extra temperature dependence of the strength  $\epsilon$  of the mean-field potential.